

Nannofossil Diversity and Climate Change of Rembang Zone, North East Java Basin

Siti Umiyatun Choiriah^{a,*}, Dwi Fitri Yudiantoro^a, Rubiyanto Kapid^b

^a Department of Geology Engineering, Faculty of Mineral Technology, UPN "Veteran" Yogyakarta, Yogyakarta, Indonesia

^b Faculty of Earth Sciences and Technology, Institut Teknologi Bandung, Bandung, Indonesia

Corresponding author: *umiyatunch@upnyk.ac.id

Abstract—This study was conducted in the Blora Regency District. This study aims to comprehensively examine the diversity of nannofossil species and their significance to climate change from the Pliocene to the Pleistocene. The rock sample was taken by spot sampling and prepared using the smear slide method. The geology area is composed of lithology containing much carbonate from the Wonocolo, Ledok, Mundu, Selorejo, and Lidah formations. The results of nannofossil analysis showed that in the Jiken area, 17 genera and 54 species were identified, Sambong had eight genera and 41 species, and Kedewan had 19 genera and 51 species. The study area is (Late Miocene/Pliocene to Pleistocene). Age of Jiken is (CNM11-CNPL7) or (10.79Ma-1.71Ma); Sambong (CNM13-CNPL8) or (9.65Ma-1.93Ma) and Kedewan (CNM14-CNPL9 or 8.80M -1.14Ma). The Diversity Index (H') and Evenness/Homogeneity Index (E) for Jiken are H' (2.551) and E (0.422), Sambong area is H' (2.280) and E (0.377) and Kedewan (H'2.344 and E 0.388). The index ranges from H'(2.280-2.251), which means small to medium diversity and moderate community stability; for index E (0.377-0.42), the nannofossil population is small to medium. These results indicate that the dominance of species abundance and diversity increased during the Miocene-Pliocene and decreased during the Pleistocene. Climate change has had a significant impact on the life of nannofossils; it has been shown that during the Pliocene (warm period), the number of nannofossils showed high diversity and abundance, and during the Pleistocene (cold), it resulted in a decrease in diversity and abundance.

Keywords—Age; climate; diversity; nannofossil.

Manuscript received 27 May 2024; revised 23 Dec. 2024; accepted 18 Jan. 2025. Date of publication 28 Feb. 2025.
IJASEIT is licensed under a Creative Commons Attribution-Share Alike 4.0 International License.



I. INTRODUCTION

Nannoplankton is an organism that belongs to the group of marine algae called coccolithophore. Coccolithophores themselves come from the haptophyta group of algae. A typical haptophyte is a small unicellular eukaryotic organism, measuring 2–20 μm in length, and is usually covered by organic or mineralized scales [1], [2]. Calcareous nannofossils are crucial for dating marine sediments due to their abundance, taxonomic diversity, rapid evolution, wide distribution, and better preservation than planktonic foraminifers [2]. Variations in orbital geometry can influence and distribute specific marine biota such as coccolithophores and unicellular phytoplankton (nannofossils), which are valid tools in geology to infer changes in surface air conditions and coccolithophore productivity and how orbital variations may affect them [3]. Nannofossils can be divided into three forms: 1. Coccolith, simple circle, ring, or oval shape, 2. Noncoccolith, varied regular shapes such as stem, star, flower, horseshoe, square etc, 3. Nannolith, irregular shape [5] (Figure 1).

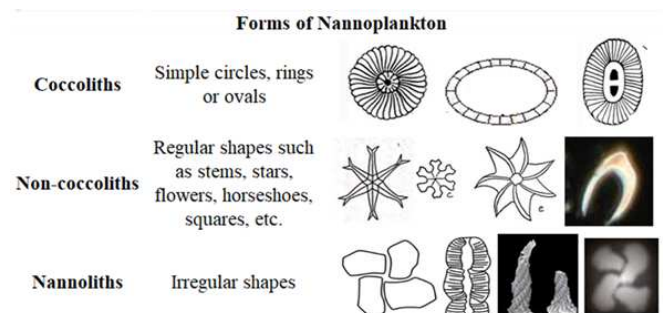


Fig. 1 Form of nannofossils [4]

Under cross-polarized light, the entire nannolith acts as a single crystal unit, though morphologically it consists of three blades [6]. The distribution and evolution of these groups of marine organisms have significant value in various research domains, including marine biology, marine geology, paleontology, and biogeochemistry [7]. Nannofossil was commonly used to indicate biostratigraphy and biodiversity

[7]. They can be employed for biostratigraphic correlation and reconstruction of geological models in hydrocarbon exploration [8], [9], [10].

The Neogene was a period of significant global climatic, floral, and faunal changes. Recently, the Miocene-Pliocene Epoch has drawn attention for its insights into climate sensitivity to CO₂ and future temperature rise predictions. [11]. As valuable indicators of global climate change [12], [13], [14], nannofossil assemblages can be used as indicators of ancient migrations and characterization to indicate ancient migrations and characterize subtropical convergence zone regimes. Nannofossils are utilized in both biostratigraphic and paleoenvironmental/paleoclimatic research. They offer the highest biostratigraphic resolution in Mediterranean regions, with an average resolution of 0.25 million years during the late Gelasian-Calabrian period [15]. These organisms respond rapidly to orbital and suborbital climate shifts, particularly since the Middle Pleistocene, especially in the Mediterranean, where such changes are notably intensified [16].

Its characteristics are warm and cold water species, dominated by *Calcidiscus leptoporus*, *Emiliania huxleyii*, *Florisphaera profunda*, and *Gephyrocapsa muelleriae* [17]. Analysis of inorganic geochemical data (oxygen isotopes) on nannofossils supports interpreting paleoenvironmental conditions and indicators of dominant climate conditions [18]. Nannofossil diversity can also be used to reconstruct the paleoenvironmental evolution of a region [19]. Climate change may pose a significant threat to marine habitats worldwide. For organisms in cold areas, such as the poles, species diversity decreases with decreasing latitude [20]. A high-resolution biostratigraphic analysis of Late Quaternary Cretaceous sediments indicates a low abundance of Pleistocene nannofossils in Arctic sediments [21].

Nannofossil collections can indicate a cool to temperate living environment with nutrient-rich surface water [22]. Nannoplankton evolved with changes in climate, structure, and ocean chemistry. There was an increase in biodiversity and the rate of evolution towards the Cenozoic and the Miocene (23.03–5.33 Ma), which was the period in which global warming occurred, compared to today. Nannofossil assemblages from the uppermost lower Miocene to the lowermost middle Miocene sediments indicate a strong preference for a warm tropical climate and a nutricline environment, characterized by significant variation in nutrient levels depending on depth [23]

Several experts have researched global climate change during the Pliocene-Pleistocene era, including [24]. The Mediterranean Sea presents warm water and has a rich diversity of marine biota influenced by climate change [9]. This climate change has significantly affected land and marine life [24]. Reconstructing the Pliocene to Pleistocene transition process in continental areas is challenging. Therefore, researchers often depend on marine depositional records. Research shows that nannofossil diversity decreased during the Pleistocene in the Kendeng Zone [25]. The Kendeng Zone in East Java experienced a decrease in the nannofossils diversity index during the Plio-Pleistocene period. This suggests that paleoecological changes, climate change, and ecosystem instability may have influenced the low diversity index. A low uniformity index (E) indicates that the ecosystem is less stable [25]. The development of

nannofossil research in the Rembang Zone and its application to climate change makes this research important.

This research aims to comprehensively determine the diversity of nannofossils in global climate changes from the local researchers [25]. Still, research on nannofossil diversity in the Rembang Zone has never been conducted. The author has researched nannofossil diversity in the Kendeng Zone, and the results show a correlation between climate change and nannofossil diversity. Previous researchers have never examined the nannofossil diversity of the Rembang Zone. The author has conducted a study on nannofossil diversity in the Kendeng Zone, and the results indicate a correlation between climate change and nannofossil diversity. The research was conducted in the Rembang zone to investigate potential differences in the impact of climate change on nannofossil diversity in the Kendeng Zone. This necessitated further research.

Pliocene (warm period/interglacial) to the Pleistocene (cold period/glaciation) in the Rembang Zone. The model can detect climate change, changes in sea level, stratigraphic sequences, and the evolution of hydrocarbon basins in the Rembang Zone. This research focuses on nannofossils, which have become fossils or nannofossils stored in sedimentary rocks. Research on nannofossil diversity has been carried out by many previous.

II. MATERIALS AND METHOD

One hundred seventy-one samples were taken from three locations (Figure 2). The locations were 1) Jiken or Nglebur section, Nglebur village, Jiken sub-district, Blora district, Central Java; map sheet Sambongpojok 1506-533, and coordinates/UTM 560186mE-565186mE, 9222852mN-9217852mN. 2) Sambong or Ledok section, Ledok, Sambong, Blora district, Central Java; map sheet Malo 1508-534 and Bojonegoro 1506-542; coordinates/UTM 563186mE-568186mE, 9216852mN-9221852mN.

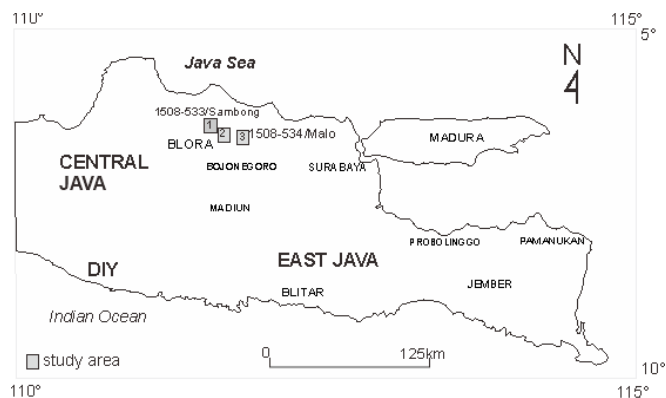


Fig. 2 Map of the research area 1. Jiken, 2. Sambong and 3. Kedewan, Blora) on the Java Island Sheet Map [26].

Location 3 was Kedewan or Banyuurip Section, Banyuurip village, Senori and Kedewan sub-districts, Tuban and Bojonegoro districts, East Java. The location can be found on map sheets Malo 1508-534 and Bojonegoro 1506-542, with coordinates/UTM ranging from 576000mE to 581000mE and 9215250mN to 9220250mN.

The object of this research used sedimentary rock samples taken from the Earth's surface with measurable stratigraphic measurements. The rock samples were particularly silt or clay

(Wentworth grain size scale) and contained carbonate minerals, as carbonates are often found as marine sediments. [27]. The size of the rock sample used for analysis is 2 grams. The samples were found in continuous sediment layers aged from the Late Miocene to the Pleistocene. From old to young, the stratigraphy includes five formations: upper Wonocolo, Ledok, Ledok, Mundu Formation, Selorejo Member, and Lidah Formation. The research involved identifying from the genus to species level and calculating the abundance and diversity of the nannofossil groups.

Species were identified according to International Standards from Nannotax3. [28], and their age was determined using the methods outlined [29] and [30]. The Shannon-Weiner Species Diversity Index was applied to estimate the number of each species present in a collection, the proportion of each species to the total number of individuals and adding up the proportion multiplied by the natural logarithm of the proportion of each species. The higher the number, the higher the species diversity [31]. The nannofossil age code consisting of letters (NN/Neogene Nannoplankton) and numbers (NN.1-NN.21) for Miocene to Pleistocene ages [29].

The different letter and number codes to identify CNM (Calcareous Nannofossil Miocene) from the Miocene (CNM11-CN20) and CNPL (Calcareous Nannofossil Plio-Pleistocene) with range (CNPL1-CNPL11) [32]. Absolute ages millions of years ago (Ma) were determined using the method described [30]. The Shannon index of diversity was applied to quantitatively calculate the number of nannofossil species present in sedimentary rocks. These indices statistically represent biodiversity in various aspects (richness, evenness, and dominance) [33], [31]. All nannofossil species were equally represented in a rock sample. The method calculates the value of P_i , representing the proportion of individuals of a particular species encountered (n_i) divided by the total number of individuals seen (N). The index uses a natural logarithm (\ln) and calculates the sum (Σ) of the number of species (S). This analysis determines the sequence of biostratigraphic zones and climate changes during the sedimentation of sedimentary rocks.

III. RESULTS AND DISCUSSIONS

A. Geological Setting

The Northeast Java region is defined by the tectonophysiology of the island of Java, which is divided into four units from south to north: Kendeng zone, Randublatung zone, Rembang zone, and Java Sea shelf. [34], [35]. The regional stratigraphy of the Rembang Zone of the East Basin shows that the rock outcrops are Late Eocene to Pleistocene. [36]

The regional geological structure of Java Island is divided into three main structural patterns, namely the Meratus pattern (Northeast-Southwest trend), the Sunda pattern (N-S trend), and the Javanese pattern (East-West trend) [36], [37]. Structures on the island of Sumatra are mainly found in West Java, while in the Eastern part of Central Java (inactive). At the same time, the Java Pattern (East-West) in the East Java basin is older than the Early Miocene (SAKALA trend) [36], [38], [39].

The lithostratigraphic units in the Rembang Zone are arranged in a sequence characterized by their composite lithology and age, as illustrated (Figure 3). Based on

nannofossil analysis, previous research suggests that locations 1, 2, and 3 are from the Late Miocene to Pleistocene (NN11-NN21) [40].

AGE		Blow Zonation	Letter classification	STRATIGRAPHY OF REMBANG ZONE			
MA				Formation	Member	Symbol of Lithology	DESCRIPTION
2	PLEISTOCENE	N23	Tgh	TRINIL			
		N22		LIDAH	TURI	Blue clay, layered marl, interbedded sandstone, lenses of coquina (meta-limestone)	
5-10	PLIOCENE	N21	Tf	TAMBAKROMO			
		N20		SELOREJO		Marl, white-grey, massive, compact, foraminiferal, with calcarenite limestone in the upper part (Selorejo)	
		N19		MUNDU			
	MIOCENE	LATE		N18	KAWENGAN	LEDOK	Sandstone, green, red, brown, glauconite, calcarenite, clay
				N17			
				N16		WONO-COLO	Marl, yellowish-brown, glauconite, calcarenite intercalations, clay
MIOCENE	MIDDLE	N15	UPPER	BULU		Calcareenite, laminated, compact glauconite	
		N14					
		N13					

Fig. 3 Stratigraphy of the upper part of Rembang Zone [40], [35]

The geology of the research area comprises the Wonocolo Formation, Ledok, Mundu, Selorejo, and Lidah Formation. These formations are Middle Miocene to Pleistocene (N13-N22) based on planktonic foraminifera (Figure 3). The study area's nannofossil analysis indicates that the ages are Late Miocene to Pleistocene or NN10-NN21 [40].

The unit is from the Middle to the Late Miocene. Above the Wonocolo Formation, the Ledok Formation (Late Miocene) limestone-calcareenite unit is deposited, namely limestone and calcarenite with layered and bioturbated sedimentary structures. Above the Ledok Formation, the Marl Unit of the Mundu Formation was deposited with a massive structure. At the top, the thin limestone Unit of the Selorejo Formation (Early Pliocene to Late Pliocene) was deposited, followed by the Lidah Formation Limestone and Siltstone Unit (Pleistocene) with a massive sedimentary structure and alluvial sedimentary units were unconformably deposited.

B. Nannofossil Analysis

Location-1, Jiken, Blora. This location comprises five formations with a total thickness of 600 meters. The lithologies consist of 69.2 meters of marl Wonocolo Formation, 297 meters of interbedded calcarenite and limestone from the Ledok Formation, 182 meters of marl Mundu Formation, 7 meters of sandstone Selorejo Formation, and 43 meters of calcareous mudstone Lidah Formation. The Selorejo limestone outcrop is a distinctive feature of this location and is absent from locations two and three. It is often associated with trace fossils and serves as a gas reservoir. The sedimentary structures include massive, laminated, parallel laminated, and cross-bedded. The results of nannofossil analyses from 70 rock samples showed 17 genera with 54 species. The species are *Amaurolithus tricorniculatus*; *Calcidiscus macintyreii*; *Calcidiscus leptopurus*, *Ceratolithus armatus*, *Ceratolithus rugosus*; *Ceratolithus cristatus*, *Coccolithus pelagicus*; *Coronociclus nitescens*; *Discoaster asymmetricus*; *Discoaster bellus*; *Discoaster berggrenii*; *Discoaster brouweri*; *Discoaster hamatus*; *Discoaster challengerii*; *Discoaster intercalaris*;

Discoaster neorectus; *Discoaster neohamatus*; *Discoaster pansus*; *Discoaster pentaradiatus*; *Discoaster prepentaradiatus*; *Discoaster quinqueramus*; *Discoaster surculus*; *Discoaster* sp.; *Discoaster triradiatus*; *Discoaster variabilis*; *Gephyrocapsa caribbeanica*; *Gephyrocapsa oceanica*; *Hayaster perplexus*; *Helicosphaera carteri*; *Helicosphaera kampteneri*; *Helicosphaera selli*; *Helicosphaera granulata*; *Helicosphaera wallichii*; *Helicosphaera macroporus*; *Oolithus fragilis*; *Ponthosphaera discopora*; *Ponthosphaera japonica*; *Ponthosphaera multipora*; *Pseudoemiliana lacunose*; *Rhabdosphaera clavigera*; *Reticulofenestra minuta*; *Reticulofenestra minutula*; *Reticulofenestra pseudoumbilicus*; *Reticulofenestra rotaria*; *Scyphosphaera apsteinii*; *Scyphosphaera globulata*; *Scyphosphaera pulcherrima*; *Sphenolithus abies*; *Sphenolithus neoabies*; *Sphenolithus compactus*; *Sphenolithus moriformis*; *Thoracosphaera saxea*; *Umbilicosphaera Jafari* (Table 1). The analysis results of the species mentioned above show the relative age of CM11-CNPL7 or Late Miocene to Pleistocene and the absolute age (10.79 - 1.71) million ages.

Location-2, Sambong, Blora. This location comprises four formations with a total thickness of 487.3 meters. The formations are composed of marl from the Wonocolo Formation, with a thickness of 69.2 meters, alternating with calcarenite limestone from the Ledok Formation (191.5 meters), marl from the Mundu Formation (128.6 meters), and greenish mudstone of the Lidah Formation (98 meters). There are no Selorejo limestone members at this location. The sedimentary structures observed are comparable to those at the Jiken location, consisting of solid layers, parallel lamination, layers, and cross-bedding.

The nannofossil analysis from 60 rock samples shows eight genera with 41 species. The species are *Calcidiscus leptopurus*; *Calcidiscus macintyreii*; *Coccolithus pelagicus*; *Discoaster variabilis*; *Discoaster neohamatus*; *Discoaster exilis*; *Discoaster bellus*; *Discoaster hamatus*; *Hayaster perplexus*; *Discoaster intercalaris*; *Discoaster challengerii*; *Discoaster asymmetricus*; *Discoaster brouweri*; *Discoaster berggrenii*; *Discoaster quinqueramus*; *Discoaster pentaradiatus*; *Discoaster surculus*; *Helicosphaera granulata*; *Helicosphaera selli*; *Helicosphaera carteri*; *Helicosphaera kampteneri*; *Helicosphaera wallichii*; *Ponthosphaera lotoculata*; *Ponthosphaera discopora*; *Ponthosphaera japonica*; *Ponthosphaera multipora*; *Reticulofenestra minutula*; *Reticulofenestra minuta*; *Reticulofenestra rotaria*; *Reticulofenestra pseudoumbilicus*; *Scyisphophaera globulata*; *Scyisphophaera pulcherrima*; *Scyisphophaera lagena*; *Scyisphophaera apsteinii*; *Scyisphophaera graphica*; *Scyisphophaera ventriosa*; *Sphenolithus moriformis*; *Sphenolithus abies*; *Sphenolithus neoabies*. (Table 1). The analysis results of the species mentioned above show the relative age is CNM13-CNPL8 (Late Miocene to Pleistocene or absolute age of (9.65 -1.93) million age.

Location-3, Kedewan, Blora. The location comprises three formations with a total thickness of 447.8 meters. These formations consist of calcarenite limestone from the Ledok Formation (207.2 meters thick), marl from the Mundu Formation (140.9 meters thick), and calcareous mudstone from the Lidah Formation (99.7 meters thick). The sedimentary structures include massive, layered, parallel lamination, cross-bedding, and bioturbation (animal tracks).

The analysis from 41 rock samples showed 19 genera with 51 species. The species are *Amaurolithus tricorniculatus*; *Ceratholithus acutus*; *Ceratholithus cristatus*; *Ceratholithus rugosus*; *Calcidiscus leptoporus*; *Calcidiscus macintyreii*; *Coronocyclus nitescens*; *Coccolithus separatus*; *Coccolithus miopelagicus*; *Coccolithus pelagicus*; *Coccolithus pliipelagicus*; *Discoaster berggrenii*; *Discoaster asymmetricus*; *Discoaster brouweri*; *Discoaster challengerii*; *Discoaster kugleri*; *Discoaster intercalaris*; *Discoaster perplexus*; *Discoaster pentaradiatus*; *Discoaster hamatus*; *Discoaster surculus*; *Discoaster* sp.; *Discoaster tristellifer*; *Discoaster variabilis*; *Emiliana huxleyi*; *Gephyrocapsa oceanica*; *Gephyrocapsa caribbeanica*; *Helicosphaera granulata*; *Helicosphaera carterii*; *Helicosphaera selli*; *Pyrocyclus hermosus*; *Ponthosphaera indoceanica*; *Ponthosphaera japonica*; *Pseudoemiliana lacunose*; *Reticulofenestra minuta*; *Reticulofenestra minutula*; *Reticulofenestra pseudoumbilicus*; *Reticulofenestra rotaria*; *Rhabdosphaera clavigera*; *Scapolithus fossilis*; *Schyposphaera apsteinii*; *Schyposphaera aranta*; *Schyposphaera globulata*; *Schyposphaera lagena*; *Schyposphaera recurvata*; *Schyposphaera ventriosa*; *Sphenolithus abies*; *Sphenolithus belemnus*; *Sphenolithus neoabies*; *Thoracosphaera saxea* and *Umbilicosphaera sibogae* (Table 1). The analysis results indicate CNM14-CNPL9 (Late Miocene to Pleistocene (8.80 -1.14) million age.

From the three locations in the study, it was concluded that at the Jiken Location, 17 out of 70 rock samples contained 54 species, indicating an age from the Middle Miocene to the Pleistocene or NN11-NN19. The Sambong area analysis of 60 samples showed eight genera with 41 species, summarised from the Middle Miocene to the Pleistocene (NN11-NN19). In Kedewan, 41 rock samples were collected and analyzed. The samples showed 19 genera with 51 species, ranging from the Middle Miocene to Pleistocene/NN11-NN21 (Nannofossil age classification [29]).

According to the classification of [30], the diversity of nannofossils found in the Jiken area shows a range of relative ages from the Late Miocene to the Pleistocene range CNM11-CNPL7 or absolute (10.79 -1.71)million age; for the Sambong area, it shows the relative age CNM13-CNPL8 (Late Miocene to Pleistocene) or the same as the absolute age (9.65 -1.93) million age, while the Kedewan area shows CNM14-CNPL9 (Late Miocene to Pleistocene) or the same as the absolute age (8.80 -1.14) million age.

TABLE I
THE DATA OF THE DISTRIBUTION OF NANNOFOSSIL SPECIES, DIVERSITY INDEX (H'), AND HOMOGENEITY (E) FROM JIKEN, SAMBONG, AND KEDEWAN
OF THE REMBANG ZONE

No.	Name of Species	JIKEN. BLORA			SAMBONG. BLORA			KEDEWAN. BLORA		
		ni	H'	E	ni	H'	E	ni	H'	E
1	<i>Amaurolithus tricorniculatus</i>	1	.003	.001	0	.000	.000	2	.006	.001
2	<i>Calcidiscus leptopurus</i>	73	.092	.017	7	.017	.004	31	.057	.010
3	<i>Calcidiscus macintyreii</i>	33	.050	.010	18	.037	.008	35	.063	.011
4	<i>Ceratholithus acutus</i>	0	.000	.000	0	.000	.000	1	.003	.001
5	<i>Ceratholithus rugosus</i>	3	.000	.000	0	.000	.000	4	.011	.002
6	<i>Ceratholithus armatus</i>	1	.003	.001	0	.000	.000	0	.000	.000
7	<i>Ceratholithus cristatus</i>	2	.005	.001	0	.000	.000	0	.000	.000
8	<i>Coccolithus miopelagicus</i>	0	.000	.000	0	.000	.000	28	.053	.010
9	<i>Coccolithus pelagicus</i>	77	.096	.018	48	.080	.018	38	.067	.012
10	<i>Coccolithus pliopelagicus</i>	0	.000	.000	10	.023	.005	9	.021	.004
11	<i>Coccolithus separatus</i>	3	.000	.000	0	.000	.000	5	.013	.002
12	<i>Coronocyclus nitescens</i>	63	.082	.016	0	.000	.000	12	.027	.005
13	<i>Discoaster asymmetricus</i>	13	.024	.005	8	.019	.004	13	.029	.005
14	<i>Discoaster bellus</i>	1	.003	.001	15	.032	.007	0	.000	.000
15	<i>Discoaster berggrenii</i>	4	.009	.002	11	.025	.006	0	.000	.000
16	<i>Discoaster brouweri</i>	56	.076	.014	38	.067	.015	32	.059	.011
17	<i>Discoaster challengerii</i>	0	.000	.000	2	.006	.001	0	.000	.000
18	<i>Discoaster exilis</i>	0	.000	.000	15	.032	.007	0	.000	.000
19	<i>Discoaster hamatus</i>	0	.000	.000	6	.015	.003	1	.003	.001
20	<i>Discoaster intercalaris</i>	1	.003	.001	1	.003	.001	3	.009	.002
21	<i>Discoaster neohamatus</i>	1	.003	.001	22	.044	.010	0	.000	.000
22	<i>Discoaster pansus</i>	1	.003	.001	0	.000	.000	0	.000	.000
23	<i>Discoaster pentaradiatus</i>	15	.027	.005	11	.025	.006	31	.057	.010
24	<i>Discoaster perplexus</i>	34	.052	.010	24	.047	.011	48	.080	.014
25	<i>Discoaster quinqueringus</i>	12	.022	.004	6	.015	.003	0	.000	.000
26	<i>Discoaster sp</i>	1	.003	.001	0	.000	.000	6	.015	.003
27	<i>Discoaster surculus</i>	7	.014	.003	6	.015	.003	10	.023	.004
28	<i>Discoaster triradiatus</i>	5	.011	.002	0	.000	.000	0	.000	.000
29	<i>Discoaster tristellifer</i>	0	.000	.000	0	.000	.000	2	.006	.001
30	<i>Discoaster variabilis</i>	10	.019	.004	15	.032	.007	5	.013	.002
31	<i>G.caribbeanica</i>	12	.022	.004	0	.000	.000	5	.013	.002
32	<i>G.oceanica (ilumina.cold)</i>	1	.003	.001	0	.000	.000	1	.003	.001
33	<i>G.small</i>	68	.087	.017	0	.000	.000	0	.000	.000
34	<i>H.macroporus</i>	2	.005	.001	0	.000	.000	0	.000	.000
35	<i>H.wallichi</i>	26	.042	.008	0	.000	.000	0	.000	.000
36	<i>Helicosphaera carterii</i>	29	.046	.009	32	.059	.013	60	.094	.017
37	<i>Helicosphaera granulata</i>	0	.000	.000	10	.023	.005	2	.006	.001
38	<i>Helicosphaera selli</i>	58	.078	.015	17	.036	.008	38	.067	.012
39	<i>Helicosphaera wallichi</i>	0	.000	.000	10	.023	.005	0	.000	.000
40	<i>Oo.fragilis</i>	36	.054	.010	0	.000	.000	0	.000	.000
41	<i>Ponthosphaera discopora</i>	34	.052	.010	18	.037	.008	0	.000	.000
42	<i>Ponthosphaera indoceanica</i>	0	.000	.000	10	.023	.005	18	.037	.007
43	<i>Ponthosphaera japonica</i>	11	.021	.004	19	.039	.009	24	.047	.009
44	<i>Ponthosphaera multipora</i>	1	.003	.001	3	.009	.002	0	.000	.000
45	<i>Pseudoemiliania lacunosa</i>	88	.105	.020	0	.000	.000	5	.013	.002
46	<i>Reticulofenestra minuta</i>	601	.325	.061	789	.366	.082	360	.288	.052
47	<i>Reticulofenestra minutula</i>	445	.286	.054	446	.316	.071	322	.273	.050
48	<i>Reticulofenestra pseudoumbicus</i>	115	.127	.024	163	.185	.042	64	.098	.018
49	<i>Reticulofenestra rotaria</i>	0	.000	.000	7	.017	.004	25	.048	.009
50	<i>Rhabdosphaera clavigera</i>	15	.027	.005	0	.000	.000	4	.011	.002
51	<i>Scapolithus fossilis</i>	0	.000	.000	0	.000	.000	15	.032	.006
52	<i>Schyposphaera apsteini</i>	9	.018	.003	1	.003	.001	6	.015	.003
53	<i>Schyposphaera aranta</i>	0	.000	.000	0	.000	.000	2	.006	.001
54	<i>Schyposphaera globulata</i>	16	.028	.005	8	.019	.004	0	.000	.000
55	<i>Schyposphaera graphica</i>	0	.000	.000	3	.009	.002	0	.000	.000
56	<i>Schyposphaera lagena</i>	0	.000	.000	2	.006	.001	1	.003	.001
57	<i>Schyposphaera pulcherrima</i>	7	.014	.003	3	.009	.002	0	.000	.000
58	<i>Schyposphaera recurvata</i>	0	.000	.000	1	.003	.001	1	.003	.001
59	<i>Schyposphaera ventriosa</i>	0	.000	.000	1	.003	.001	3	.009	.002
60	<i>Sphenolithus moriformis</i>	0	.000	.000	60	.094	.021	0	.000	.000
61	<i>Sphenolithus abies</i>	452	.288	.055	278	.253	.057	347	.283	.051
62	<i>Sphenolithus belemnos</i>	0	.000	.000	0	.000	.000	4	.011	.002
63	<i>Sphenolithus neo abies</i>	488	.298	.056	203	.212	.047	721	.363	.066
64	<i>Thoracosphaera saxea</i>	4	.009	.002	0	.000	.000	2	.006	.001
65	<i>Umbilicosphaera jafari</i>	3	.007	.001	0	.000	.000	0	.000	.000
		2935	2.551	.422	2347	2.280	.377	2346	2.344	.388
			44		36			36		

C. Climate change of Pliocene to Pleistocene

Pliocene Climate Change is known as global temperature, but some studies show warm conditions during the Pliocene. This is still the case, whether there is a permanent El Nino effect or not. Indonesia is a prime location for studying past to present climate. Several Pliocene climate studies have been conducted in Indonesia based on pollen content analysis, and the results show the existence of warm climate conditions during the late Pliocene [41]. In the late Pliocene and Pleistocene, maximum glaciation occurred, and faunal migration to Java occurred during the Early Pleistocene. [42]

The collection of calcareous nannofossils indicates warm air conditions, which is indicated by the dominance of *Sphenoliths* (*Sphenolithus* spp.) [43].

The global decline of the nannofossil genus *Discoaster* is associated with decreased sea surface temperature and increased climate variability, and it has been reported that this decline is observed mainly in cold climates [44]. A comparison of the abundance and diversity of nannofossils at three locations with an interpretation of climate change is presented in the graph (Figure 4).

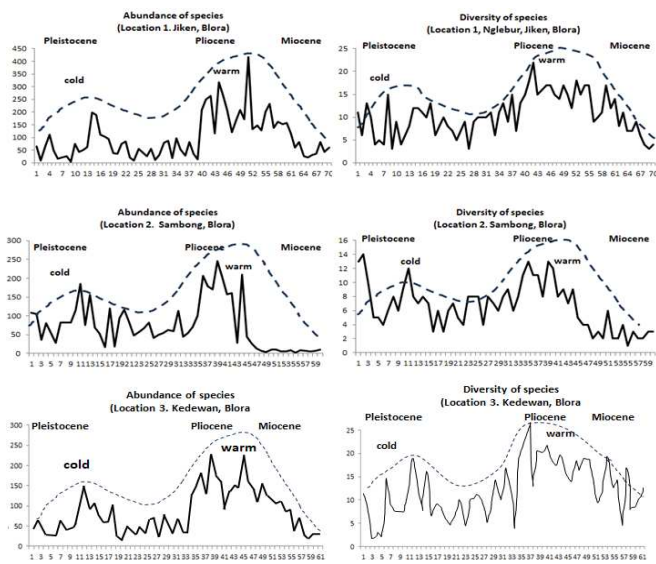


Fig. 4 Data on the abundance and diversity of nannofossils at three locations and interpretation of climate change

Based on data analysis and diversity at each location, differences in reporting patterns and nannofossil diversity can be observed in each rock. All locations' abundance and diversity results show the same graph (red line). The data is at its lowest in the Late Miocene, then it increases in the Pliocene and decreases again in the Plio-Pleistocene (interglacial). The Pleistocene Era is often accompanied by an ice age where the Earth experienced global cooling. The data suggest climate change factors impact the reporting and diversity of nannofossils (Figures 5, 6, and 7).

An analysis of the results of the summarizing index and nannofossil diversity supports this data. This data shows a relatively decreasing pattern of older rocks, especially the Pliocene, and a decline in the Pleistocene age. Environmental factors may have caused the difference in this index during the Pliocene age, which had relatively warm temperatures, sufficient nutrition, and salinity that were suitable for the life

of nannofossil. Conversely, the Pleistocene age had relatively cold temperatures, which were not preferable for many sensitive nannofossils, resulting in their eventual death (Figures 5, 6, and 7).

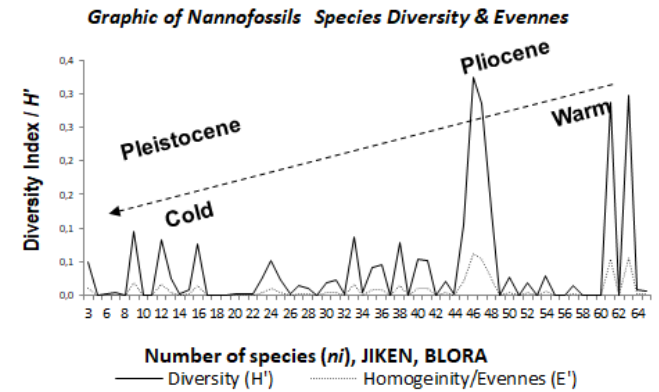


Fig. 5 The Pliocene-Pleistocene diversity model of nannofossil species from Jiken, Blora.

An analysis of the results of the summarizing index and nannofossil diversity supports this data. This data shows a relatively decreasing pattern of older rocks, especially the Pliocene, and a decline in the Pleistocene age. Environmental factors may have caused the difference in this index during the Pliocene age, which had relatively warm temperatures, sufficient nutrition, and salinity that were suitable for the life of nannofossil. Conversely, the Pleistocene age had relatively cold temperatures, which were not preferable for many sensitive nannofossils, resulting in their eventual death (Figures 5, 6, and 7).

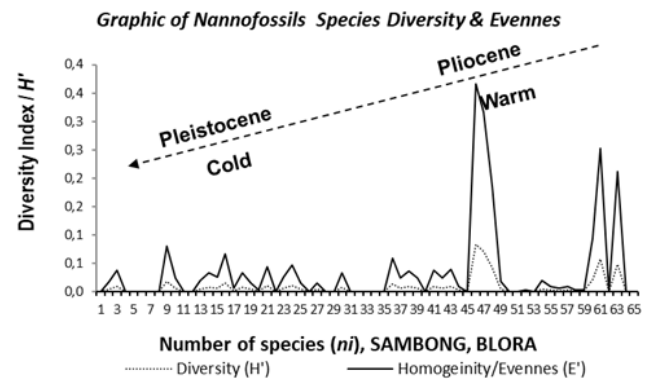


Fig. 6 The Pliocene-Pleistocene diversity model of nannofossil species from Sambong, Blora

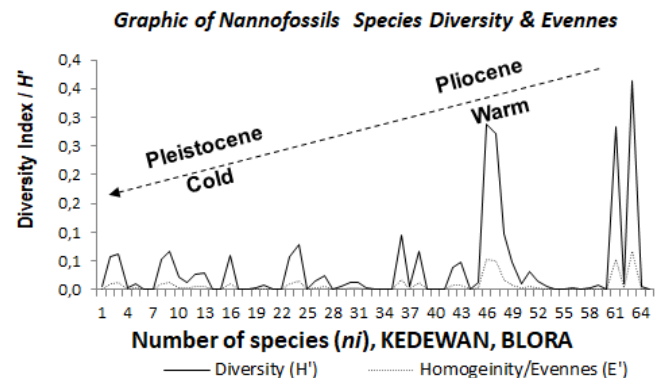


Fig. 7 The Pliocene-Pleistocene diversity model of nannofossil species from Kedewan, Blora

The interpretation of climate change: Based on the three abundance graphs and three nannofossil diversity graphs, the understanding of climate change reveals a consistent pattern across all three locations. The results indicate decreased abundance and diversity values during the Pliocene age. The graph illustrates a consistent pattern, supported by analysis of diversity and evenness/homogeneity index data, indicating that climate change significantly impacts the life of nannofossil at that age. During warm climate periods, nannofossils exhibit high diversity and abundance; during cold climate periods, their numbers decrease, resulting in low diversity and abundance.

IV. CONCLUSION

The results of nannofossil analysis at three locations, namely in the Jiken area, identified 17 genera with 54 species, with the age of CM11-CNPL7 or Late Miocene to Pleistocene with an absolute age of 10.79 Ma -1.71 Ma. The Sambong area identified eight genera and 41 species, ranging from Late Miocene to Pleistocene or CNM13-CNPL8 or absolute age (9.65 Ma -1.93 Ma). The Kedewan area contains 19 genera with 51 species, showing an age from CNM14-CNPL9 or Late Miocene to Pleistocene, with an absolute age (8.80 Ma - 1.14 Ma).

The Diversity Index (H') of Jiken is 2.551 (medium diversity and moderate community stability), while the Evenness/Homogeneity Index (E) of 0.422 shows a moderate population. The Sambong Diversity Index (H') is 2,280 (small diversity and Low Community stability), while the Evenness Index (E) is 0.377 (small population). The Diversity Index (H') of the Kedewan is 2.344 (medium diversity and moderate community stability, and the Evenness Index (E) of 0.388 shows a small population. The range of the nannofossil (H') is 2.280 to 2.251, which indicates small to moderate diversity and moderate community stability. The Homogeneity (E) range is 0.377 to 0.42, indicating a small to medium population size. A smaller diversity index (H') value indicates a lower uniformity index (E), which means the dominance of a particular species over other species. The abundance and diversity of species increased during the Miocene and decreased during the Pleistocene.

Based on the data, the abundance and diversity of nannofossil in the Miocene age is higher than in the Pleistocene. This data shows that the abundance and diversity values of nannoplankton are influenced by climate change; in other words, climate change has a significant impact on the life of nannoplankton, whereas in the Miocene/Pliocene (warm period), nannofossils show high diversity and abundance; Meanwhile, during the Pleistocene (cold period), the diversity and abundance of nannofossil decreased.

NOMENCLATURE

Fossil age range code by Backman et, 2015

CNM	Calcareous Nannofossil Miocene
CNPL	Calcareous Nannofossil Plio-Pleistocene
NN	Neogene Nannofossil by Martini, 1971
N	Neogene (based on foraminifera) by Blow, 1969
H'	The Diversity Index
E	Evenness/Homogeneity Index

Subscripts

Ma	Million age	
um	size of microfossil	micron
mE	map coordinate	meter East
mN	map coordinate	meter North

ACKNOWLEDGMENT

The author would like to thank LPPM UPN VY for providing internal research funding assistance, Dr. Ir. C. Prasetyadi, M.Sc., for his discussion, and thanks to the Rembang Team research assistants (Nanda Ajeng, Bramantyo, and Ariq Fadhilah) who have helped in the field.

REFERENCES

- [1] M. Penot, J. B. Dacks, B. Read, and R. G. Dorrell, "Genomic and meta-genomic insights into the functions, diversity and global distribution of haptophyte algae," *Appl. Phycol.*, vol. 3, no. 1, pp. 340–359, Dec. 2022, doi: 10.1080/26388081.2022.2103732.
- [2] I. Raffi and J. Backman, "The role of calcareous nannofossils in building age models for Cenozoic marine sediments: a review," *Rend. Lincei. Sci. Fis. e Nat.*, vol. 33, no. 1, pp. 25–38, Mar. 2022, doi:10.1007/s12210-022-01048-x.
- [3] M. Bordiga, C. Lupi, R. Sacchi, P. Ferretti, S. J. Crowhurst, and M. Cobianchi, "Eccentricity signal in the nannofossil time-series across the Mid-Pleistocene Transition in the northwestern Pacific Ocean (ODP Site 1209)," *Quat. Sci. Rev.*, vol. 316, p. 108253, Sep. 2023, doi:10.1016/j.quascirev.2023.108253.
- [4] P. R. Bown, J. A. Lees, and J. R. Young, "Calcareous nannoplankton evolution and diversity through time," *Coccolithophores*, pp. 481–508, 2004, doi: 10.1007/978-3-662-06278-4_18.
- [5] M. Widhiyatmoko, Vijaya Isnaniawardhani, and Moh Heri Hermiyanto Zajuli, "Distribusi Nannofosil dan Foraminifera pada Batas Pliosen-Plistosen Formasi Batilembuti di Pulau Yamdena, Provinsi Maluku dan Relevansinya dengan Tektonik Regional," *J. Geol. dan Sumberd. Miner.*, vol. 24, no. 1, pp. 39–50, Feb. 2023, doi:10.33332/jgsm.geologi.v24i1.737.
- [6] C. Lancis, J.-E. Tent-Manclús, and J.-A. Flores, "Origin and evolution of the Neogene calcareous nannofossil *Ceratolithus*," *Mar. Micropaleontol.*, vol. 186, p. 102310, Jan. 2024, doi:10.1016/j.marmicro.2023.102310.
- [7] U. Ciołko and E. Gaździcka, "Calcareous nannofossil biostratigraphy and paleogeographic significance in the lower Maastrichtian of the Miechów Trough (southern Poland)," *Acta Geol. Pol.*, vol. 72, no. 3, pp. 331–352, 2022, doi: 10.24425/app.2022.140428.
- [8] S. Senemari and A. Mejía-Molina, "Nannoplankton and ^{13}C and ^{13}O stable isotope stratigraphy record of the mid Cretaceous sequences, Zagros Basin (western Iran)," *Mar. Pet. Geol.*, vol. 128, p. 105055, Jun. 2021, doi: 10.1016/j.marpetgeo.2021.105055.
- [9] S. Jan et al., "Impact of Climate Change on Marine Biodiversity: Current Challenges and Future Perspectives," *Proc. Pakistan Acad. Sci. Part B*, vol. 60, no. 1, pp. 29–47, 2023, doi: 10.53560/PPASB(60-1)768.
- [10] C. A. Setyaningsih, D. Kurniadi, T. B. S. Rasantyo, I. Firdaus, and I. Prayitno, "Planktonic and benthic foraminiferal stable isotopes, SSTs and thermocline temperature, coccoliths and benthic foraminiferal assemblages, and productivity reconstr.," *Simp. IATMI 2022*, 2022.
- [11] A. Chakraborty, A. K. Ghosh, S. Saxena, R. Dey, and L. Roy, "Neogene biostratigraphy and paleoceanography of Andaman and Nicobar Basin: A reappraisal," 2023, pp. 121–187. doi:10.1016/bs.sats.2023.08.005.
- [12] V. Isnaniawardhani, M. Rivaldy, Ismawan, R. I. Sophian, and A. S. Andyastiya, "The Miocene (25.2 – 5.6 million years ago) climate changes recorded by foraminifera and nannofossils assemblages in Bogor Basin, Western Java," *IOP Conf. Ser. Earth Environ. Sci.*, vol. 575, no. 1, p. 012222, Oct. 2020, doi: 10.1088/1755-1315/575/1/012222.
- [13] M. late. Sam, B. Paul, J. T. Richard, D. Silvia, and V. Vivi, "Global record of 'ghost' nannofossils reveals plankton resilience to high CO₂ and warming," *Science (80-.)*, vol. 376, no. 6595, pp. 853–856, 2022, doi: 10.1126/science.abm7330.
- [14] M. Arundhathy, R. Jyothibabu, S. Santhikrishnan, K. J. Albin, S. Parthasarathi, and C. P. Rashid, "Coccolithophores: an

- environmentally significant and understudied phytoplankton group in the Indian Ocean,” *Environ. Monit. Assess.*, vol. 193, no. 3, p. 144, Mar. 2021, doi: 10.1007/s10661-020-08794-1.
- [15] S. Bonomo *et al.*, “Calcareous Nannofossil variability controlled by Milankovitch and sub-Milankovitch periodicity in the Monte San Nicola section (Gelasian GSSP / MIS 100–104),” *Mar. Micropaleontol.*, vol. 192, p. 102397, Sep. 2024, doi:10.1016/j.marmicro.2024.102397.
- [16] A. Incarbona *et al.*, “Middle-Late Pleistocene Eastern Mediterranean nutricline depth and coccolith preservation linked to Monsoon activity and Atlantic Meridional Overturning Circulation,” *Glob. Planet. Change*, vol. 217, p. 103946, Oct. 2022, doi:10.1016/j.gloplacha.2022.103946.
- [17] C. Yu, X. Su, X. Ding, J. Zhang, C. Tao, and S. Lv, “Calcareous nannofossil records and the migration of the Agulhas Return Current during the last 40 kyr,” *Front. Earth Sci.*, vol. 12, May 2024, doi:10.3389/feart.2024.1322023.
- [18] N. Omar, T. McCann, A. I. Al-Juboury, M. A. Ustinova, and A. O. Sharezwri, “Early Jurassic–Early Cretaceous Calcareous Nannofossil Biostratigraphy and Geochemistry, Northeastern Iraqi Kurdistan: Implications for Paleoclimate and Paleocological Conditions,” *Geosciences*, vol. 12, no. 2, p. 94, Feb. 2022, doi:10.3390/geosciences12020094.
- [19] A. Nyerges, Á. T. Kocsis, and J. Pálffy, “Changes in calcareous nannoplankton assemblages around the Eocene-Oligocene climate transition in the Hungarian Palaeogene Basin (Central Paratethys),” *Hist. Biol.*, vol. 33, no. 9, pp. 1443–1456, 2021, doi:10.1080/08912963.2019.1705295.
- [20] M. Olofsson and A. Wulff, “Looking back to the future—micro- and nanoplankton diversity in the Greenland Sea,” *Mar. Biodivers.*, vol. 51, no. 4, 2021, doi: 10.1007/s12526-021-01204-w.
- [21] M. J. Razmjooei *et al.*, “Revision of the Quaternary calcareous nannofossil biochronology of Arctic Ocean sediments,” *Quat. Sci. Rev.*, vol. 321, p. 108382, Dec. 2023, doi:10.1016/j.quascirev.2023.108382.
- [22] C. M. Lowery, P. R. Bown, A. J. Fraass, and P. M. Hull, “Ecological Response of Plankton to Environmental Change: Thresholds for Extinction,” *Annu. Rev. Earth Planet. Sci.*, vol. 48, pp. 403–429, 2020, doi:10.1146/annurev-earth-081619-052818.
- [23] A. Chakraborty, A. K. Ghosh, and S. Saxena, “Neogene calcareous nannofossil biostratigraphy of the northern Indian Ocean: Implications for palaeoceanography and palaeoecology,” *Palaeogeogr. Palaeoclimatol. Palaeoecol.*, vol. 579, p. 110583, Oct. 2021, doi:10.1016/j.palaeo.2021.110583.
- [24] M. Dröllner *et al.*, “Directly Dating Plio-Pleistocene Climate Change in the Terrestrial Record,” *Geophys. Res. Lett.*, vol. 50, no. 8, pp. 1–10, 2023, doi: 10.1029/2023GL102928.
- [25] S. U. Choiriah, C. Prasetyadi, R. Kapid, and D. F. Yudiantoro, “Diversity model of Pliocene-Pleistocene nannofossil of Kendeng Zone,” *IOP Conf. Ser. Earth Environ. Sci.*, vol. 212, no. 1, 2018, doi:10.1088/1755-1315/212/1/012038.
- [26] A. Anonim, “Peta Rupa Bumi Indonesia (RBI) dan Peta Kontur. Jawa Timur,” Badan Informasi Geospasial (BIG). [Online]. Available: <https://www.indonesia-geospasial.com/search/label/BIG-RBI?&max-results=8>.
- [27] A. V. Turchyn, H. J. Bradbury, K. Walker, and X. Sun, “Controls on the Precipitation of Carbonate Minerals Within Marine Sediments,” *Front. Earth Sci.*, vol. 9, Feb. 2021, doi: 10.3389/feart.2021.618311.
- [28] S. Kanungo, J. Young, and G. Skowron, “Microfossils: Calcareous Nannoplankton (Nannofossils),” 2017, pp. 1–18. doi: 10.1007/978-3-319-02330-4_4-1.
- [29] E. Martini, “Standard Tertiary and Quaternary Calcareous Nannoplankton Biozonation,” in *Nannofossil Biostratigraphy*, Hutchinson Ross Publishing Company, 1971, pp. 264–307.
- [30] J. Backman, I. Raffi, D. Rio, E. Fornaciari, and H. Pälke, “Biozonation and biochronology of Miocene through Pleistocene calcareous nannofossils from low and middle latitudes,” *Newsletters Stratigr.*, vol. 45, no. 3, pp. 221–244, Nov. 2012, doi: 10.1127/0078-0421/2012/0022.
- [31] K. A. Nolan and J. E. Callahan, “Beachcomber Biology: The Shannon-Weiner Species Diversity Index This article reprinted from: Visit ABLE on the Web at :,” *Estud. Lab. Teach.*, vol. 27, no. January 2006, pp. 334–338, 2015.
- [32] I. Raffi, C. Agnini, J. Backman, and R. Catanzariti, “A Cenozoic calcareous nannofossil biozonation from low and middle latitudes: A synthesis,” vol. 36, no. 2, pp. 121–132, 2016.
- [33] C. E. Shannon and W. Weaver, “The Theory of Mathematical Communication,” *Bell Syst. Tech. J.*, vol. 27, pp. 379–429, 1964.
- [34] S. U. Choiriah, C. Prasetyadi, D. F. Yudiantoro, R. Kapid, and N. A. Nurwantari, “Miocene to pleistocene biostratigraphy of Rembang Zone based on nannofossil, Nglebur River section, Blora, Central Java,” *AIP Conf. Proc.*, vol. 2245, pp. 1–11, 2020, doi: 10.1063/5.0006851.
- [35] S. U. Choiriah, I. P. Haty, and E. Y. Kaesti, “Sedimentation Rate During Miocene to Pleistocene Related with Nannofossil Biostratigraphy, in Banyuurip, Kedewan, Rembang Zone, East Java Basin, Indonesia,” *Indones. J. Geosci.*, vol. 10, no. 3, pp. 349–361, 2023, doi: 10.17014/ijog.10.3.349-361.
- [36] A. H. Satyana, “Subvolcanic Hydrocarbon Prospectivity of Java: Opportunities and Challenges,” in *Proc. Indonesian petrol. Assoc., 39th Ann. Conv.*, Jakarta: Indonesian Petroleum Association (IPA), 2015. doi: 10.29118/IPA.0.15.G.105.
- [37] J. Ivana, L. Supriatna, and T. R. P. Astuti, “Identification of Potential Groundwater Recharge Zone Using Remote Sensing and GIS in Upstream Cibeet Sub-watershed, Bogor, West Java,” *IOP Conf. Ser. Earth Environ. Sci.*, vol. 1111, no. 1, p. 012025, Dec. 2022, doi:10.1088/1755-1315/1111/1/012025.
- [38] E. S. Sitingjak, B. Sapiie, A. M. Ramdhan, A. N. Hidayati, Y. A. Azhari, and N. F. Adriyansyah, “Surface Geology Analysis on the Relationship between Fault Creep and Overpressure in Grobogan, Central Java, Indonesia,” *IOP Conf. Ser. Earth Environ. Sci.*, vol. 1245, no. 1, p. 012019, Sep. 2023, doi: 10.1088/1755-1315/1245/1/012019.
- [39] H. W. K. Berghuis *et al.*, “The eastern Kendeng Hills (Java, Indonesia) and the hominin-bearing beds of Mojokerto, a re-interpretation,” *Quat. Sci. Rev.*, vol. 295, p. 107692, Nov. 2022, doi:10.1016/j.quascirev.2022.107692.
- [40] S. U. Choiriah, C. Prasetyadi, D. F. Yudiantoro, R. Kapid, and N. A. Nurwantari, “Miocene to Pleistocene Biostratigraphy of Rembang Zone based on nannofossil, Nglebur River section, Blora, Central Java,” *AIP Conf. Proc.*, vol. 2245, pp. 1–11, 2020, doi: 10.1063/5.0006851.
- [41] V. C. Agusta, M. Hendrizan, S. Y. Cahyarini, D. A. Utami, and A. U. Nurhidayati, “Pliocene climate in Indonesia: a review,” *IOP Conf. Ser. Earth Environ. Sci.*, vol. 789, no. 1, p. 012054, Jun. 2021, doi:10.1088/1755-1315/789/1/012054.
- [42] M. S. Omar *et al.*, “Peatlands in Southeast Asia: A comprehensive geological review,” *Earth-Science Rev.*, vol. 232, p. 104149, Sep. 2022, doi: 10.1016/j.earscirev.2022.104149.
- [43] Y. V. Vernyhorova *et al.*, “The Miocene Climatic Optimum at the interface of epicontinental sea and large continent: A case study from the Middle Miocene of the Eastern Paratethys,” *Mar. Micropaleontol.*, vol. 181, p. 102231, May 2023, doi: 10.1016/j.marmicro.2023.102231.
- [44] J. D. Schueth and T. J. Bralower, “The relationship between environmental change and the extinction of the nannoplankton Discoaster in the early Pleistocene,” *Paleoceanography*, vol. 30, no. 7, pp. 863–876, 2015, doi: 10.1002/2015PA002803.